Continental Shelf Research 66 (2013) 123–135

Contents lists available at ScienceDirect

Continental Shelf Research

journal homepage: www.elsevier.com/locate/csr

Research papers

Continental shelf water masses off the Jaguaribe River (4S), northeastern Brazil

F.J.S. Dias [a,b,*], B.M. Castro [a], L.D. Lacerda [c]

[a] Instituto Oceanográfico da Universidade de São Paulo, Laboratório de Hidrodinâmica Costeira (LHiCO/IO/USP), São Paulo, SP, Brazil
[b] Departamento de Oceanografia e Limnologia da Universidade Federal do Maranhão, Laboratório de Hidrodinâmica Costeira, Estuarina e Águas Interiores (LHiCEAI/DEOLI/UFMA), São Luís, MA, Brazil
[c] Instituto de Ciências do Mar da Universidade Federal do Ceará, Laboratório de Biogeoquímica Costeira (LBC/LABOMAR/UFCE), Fortaleza, CE, Brazil

ARTICLE INFO

Article history:
Received 13 September 2012
Received in revised form
30 May 2013
Accepted 6 June 2013
Available online 26 June 2013

Keywords:
Continental shelf
Water masses
Jaguaribe River
Estuarine plume

ABSTRACT

This work analyzed temperature and salinity data obtained from two oceanographic cruises carried out over the western portion of the continental shelf adjacent to the Jaguaribe River in NE Brazil (May and October 2009) and included the rainy and dry seasons, which correspond to different levels of continental contribution to shelf waters. The results of the analysis identified three different water masses: River Water (RW), Coastal Water (CW) and Tropical Water (TW). During the period of maximum freshwater discharge, an estuarine plume that extended for 6 km along the coastline was observed, and its influence could be felt over the inner shelf. The plume was associated with the presence of CW separated by a strong halocline. However, in the middle and outer shelf regions, the CW and the TW were observed below the 50 m isobath, while the RW was not observed, most likely due to the presence of northeast trade winds that press the plume along the coast, reducing its seaward expansion. During the dry season, a higher influence of the TW was observed, most likely due to the space-time variability of the North Brazil Current (NBC) and the role of anticyclonic eddies that meander from the adjacent ocean towards the continental shelf. The results obtained suggest a strong seasonal influence upon the water mixing process along the continental shelf with the CW being affected by the RW and TW depending upon the season.

1. Introduction

The Northeastern Brazilian Continental Shelf region is highly energetic due to the combined influence of a western boundary current, trade winds, tidal fluctuations and freshwater discharges from several rivers. This is a dynamically rich region and the origin of many important features of Atlantic Ocean circulation. One of those features is the eastward-flowing Equatorial Undercurrent (EUC), which is fed by the North Brazil Current (NBC) (Metcalf and Stalcup, 1967; Molinari, 1982) as it flows along the Brazilian coast near the equator. The North Equatorial Undercurrent (NEUC) is fed by the subthermocline layers of the NBC, which permanently retroflect anticyclonically between 3°N and 5°N (Cochrane et al., 1979; Molinari, 1982, 1983; Peterson and Stramma, 1990).

In recent decades, the spread *TS* diagram has been used as one of the main techniques for analysis of water masses in coastal and oceanic regions that exhibit vertical stratification of water masses involved in the processes of circulation and mixing (Bindoff et al., 2000; Emilson, 1961; Mascarenhas et al., 1971; Miranda and Castro, 1979; Miranda, 1985; Okunda, 1962). Silveira et al. (1994) observed between 3°N and 5°N a typical South Atlantic profile in which tropical water (TW) was found from the surface to 70 m depth. Between 70 and 100 m there occurred a mixed layer with water from the central South Atlantic (SACW). SACW dominated the profile to a depth of 700 m where the presence of Antarctic Intermediate Water (AAIW) was observed.

A pioneering study carried out by Garvine and Monk (1974) observed the frontal structure found along the boundary of the Connecticut River plume in Long Island Sound, naming it an estuarine plume. An estuarine plume is characterized as a horizontal extension into the ocean of a continental freshwater discharge that mixes within the coastal circulation as well as the physical properties of different water masses (Garvine, 1977). A particular case of an estuarine plume was initially described by several publications (Curtin, 1986; Curtin and Legeckis, 1986; Geyer et al., 1991) focused on the Amazon River, which has an

* Corresponding author at: Departamento de Oceanografia e Limnologia da Universidade Federal do Maranhão, Laboratório de Hidrodinâmica Costeira e Águas Interiores (LHiCEAI/DEOLI/UFMA), São Luis, MA, Brazil. Tel.: +55 98 3272 8561.
E-mail addresses: geofranzedias@gmail.com, geofranzedias@yahoo.com.br (F.J.S. Dias).

0278-4343/$ - see front matter © 2013 Elsevier Ltd. All rights reserved.
http://dx.doi.org/10.1016/j.csr.2013.06.005

average outflow of 1.8×10^5 m^3 s^{-1} that extends to the open sea. Its influence can be felt in the North Atlantic Ocean, and the plume covers thousands of square kilometers.

The continental shelf of Ceará State (CSC), Northeastern Brazil, has a shallow water depths and a gentle slope. Its waters are particularly responsive to changes in atmospheric conditions. Changes in the bathymetry and direction of the region's coastal flow associated with low continental contributions and the presence of cells of high salinity make this region a highly complex system in terms of its ecology and oceanography. A few studies have characterized the basic descriptive oceanography of the continental shelf in the Brazilian Northeast (e.g., Castro and Miranda, 1998; Dominguez, 2004; Silva and Alvarenga, 1994); most aimed to identify mesoscale processes over the Outer Continental Shelf but were unable to elucidate the subtle influences of coastal inputs and seasonality on the extents and distributions of observed water masses over the inner shelf.

The goals of the present work were to (1) evaluate the horizontal and vertical distribution of temperature and salinity over the CSC during the dry and rainy seasons, (2) determine the influence of the period of larger continental outflow on the local distribution of salinity and water masses in the continental shelf area and (3) characterize the coastal zone off the Jaguaribe River based on water mass distributions.

2. Study area

The continental shelf off the Northeastern Brazilian coast is narrow, ranging from 100 to 40 km in its extreme western and

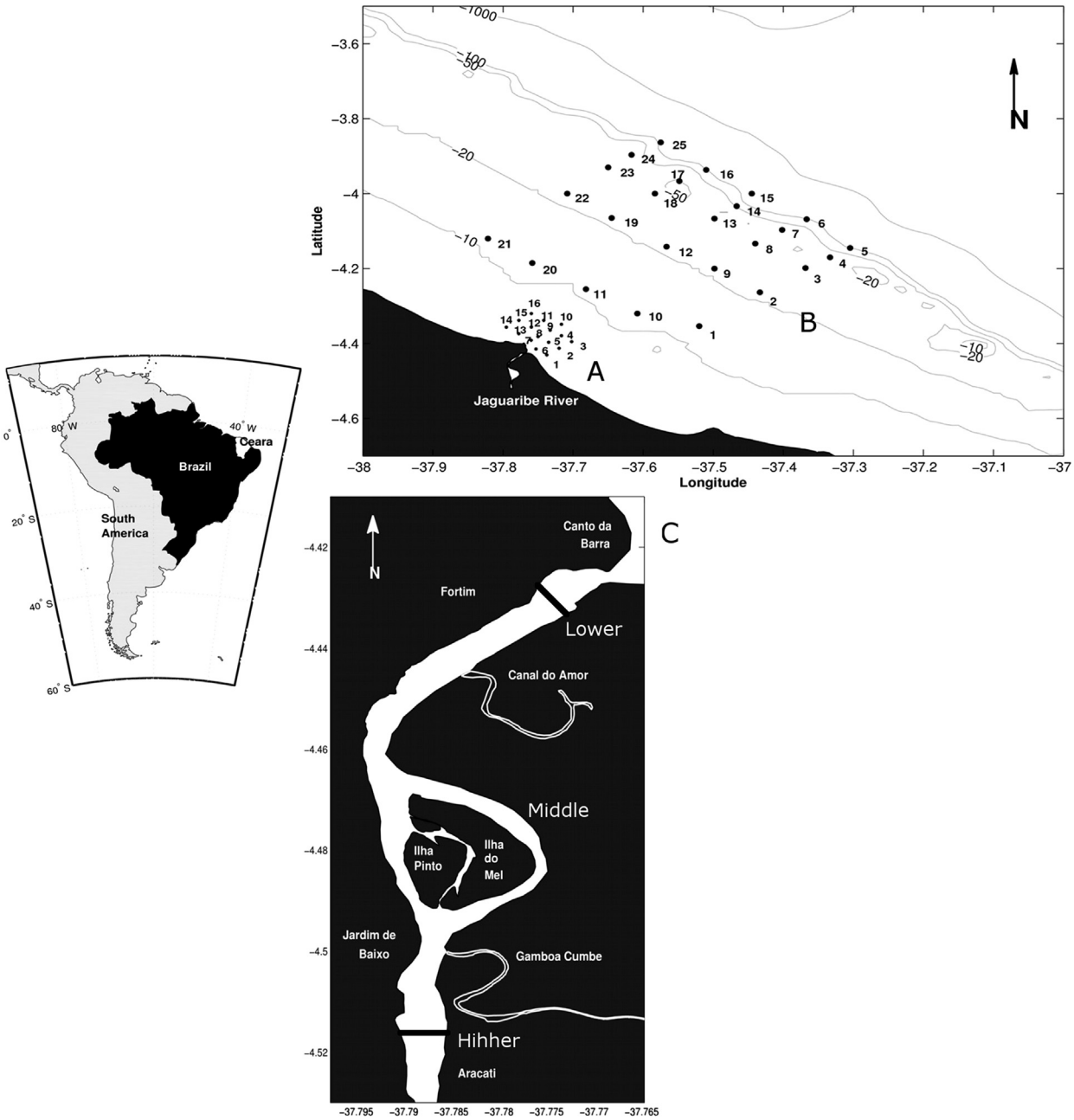

Fig. 1. Continental shelf off the Jaguaribe River. (A) Sampling grid with 16 stations arranged in five transects over the Inner Shelf off the mouth of the river. (B) Sampling grid with 25 stations arranged in five transects between 10 and 100 m isobaths over the middle and outer shelf during dry and rainy seasons. (C) The Jaguaribe River estuary where CTD data were collected over 13 h in two profiles representing the interfaces between the upper and middle and the middle and lower estuary regions (white lines) during dry and rainy seasons.

eastern regions, respectively. The shallow depth and topography are of tectonic origin and reflect the local geological conditions. The CSC off the Jaguaribe River extends over 100 km between 37° and 38°W and 3°40′ and 4°30′ S, with depths of up to 100 m and a gentle slope of 1:670 to 1:1000 to a depth of 70 m (Arz et al., 1999; Martins and Coutinho, 1981). Where the shelf is relatively narrow, coastal currents influence the coastline and are associated with relatively low tidal current influence. Two sectors are easily identified in the CSC: Sediments down to the 20 m isobath are mostly quartz sand, followed by calcareous algae to 70 m depth (Summerhayes et al., 1975). The interaction between these sediment types and the predominant climate reflects a small continental contribution due to the semi-arid climate and the small fluvial contribution (Knoppers et al., 1999).

The largest fluvial contribution to the CSC region (Fig. 1A) is from the Jaguaribe River drainage basin (Fig. 1B), responsible for approximately 50 percent of the total fluvial outflow to the continental shelf. The hydrographic network of its drainage reflects the seasonal climate in the region, where secondary rivers flow only during the rainy season. The maximum river levels are observed in February and March, coincident with the period of largest rainfall.

The semi-arid Northeastern Brazilian coast is marked by a strong seasonal rainfall regime, with two well-defined periods. The rainy season begins in December and extends to mid-June, with March and April experiencing the highest rainfall. The dry season extends from July to mid-November, and September is considered the driest month (Fig. 2A). Another determinant of the regional climate processes is the phenomenon of the trade winds, which are generated from the high-pressure South Atlantic cell and push the Inter-Tropical Convergence Zone (ITCZ) towards northeastern Brazil between December and June, during the rainy season. In the dry season, when the ITCZ moves north, wind intensity increases and exhibits an average direction of 110° (Kousky, 1980; Riehl, 1965). The powerful trade winds observed during the first semester have mean velocities of 3 to 4 m s^{-1}, whereas in the second semester mean velocities can reach 5 to 6 m s^{-1}. A force balance is observed between Coriolis and pressure gradient forces leading to a homogeneous continental shelf current with Ekman transport toward the shore piling water and generating inclination currents. The South Atlantic Subtropical Gyre and the trade winds are the main agents determining the climate in the CSC region. Soares and Castro Filho (1996) used a numerical model to study the response of water masses in the CSC

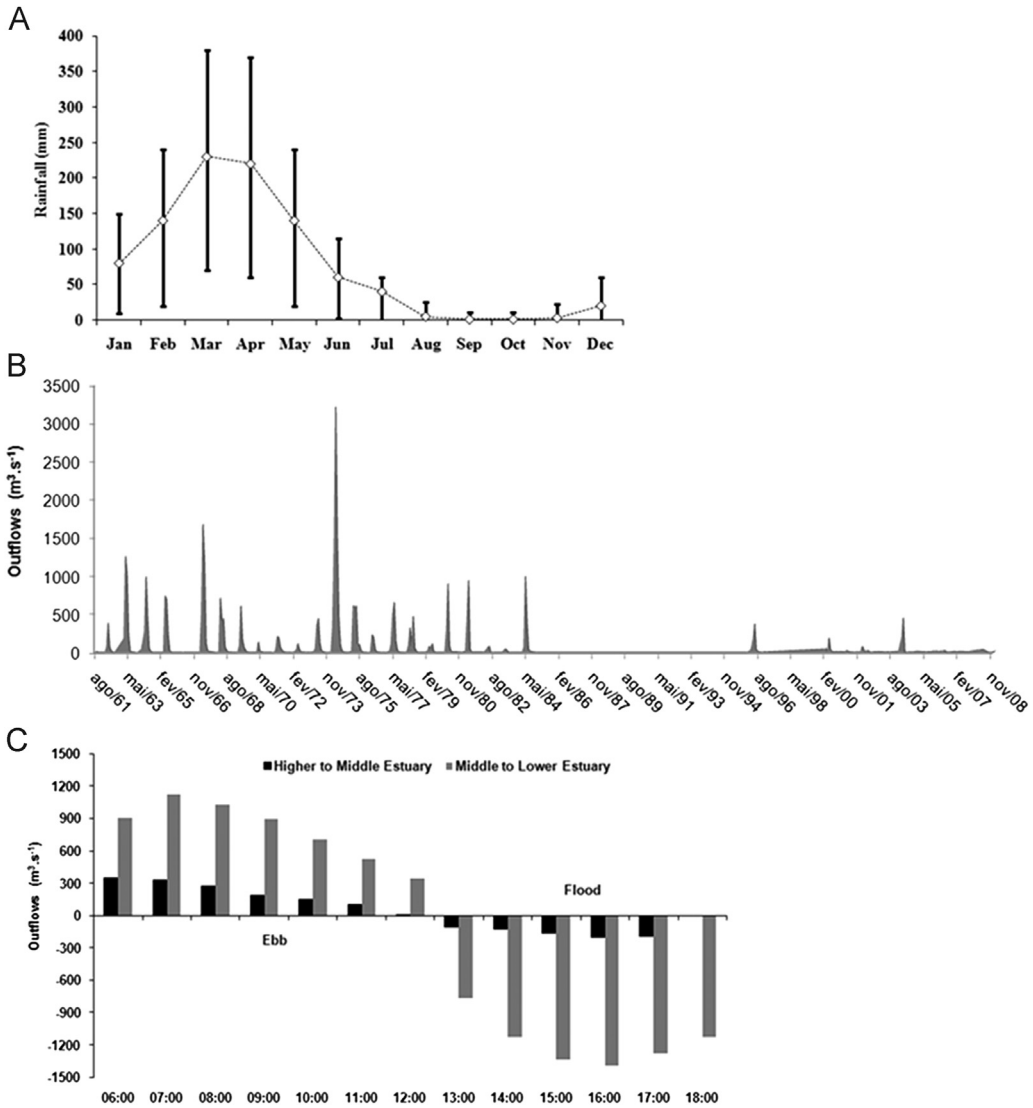

Fig. 2. Rainfall average values between 1961 and 2008 with their standard deviations (A). Historical outflow measurements by the National Water Agency (ANA) from 1961 and 2008 (B). Outflow measurements according to Dias et al. (2011) for the Jaguaribe River estuary during a spring tide (C).

region to stationary and transient winds. In this study, the authors observed that the wind shear stress had an important role in determining the circulation over the CSC and that were surface currents and elevations exhibited decays that were exponential with distance from the coast.

Historical outflow data provided by the National Water Agency of Brazil (ANA, 2008) have shown a reduction in the fluvial contribution to the continental shelf waters due to the intensification of dam construction along the Jaguaribe River basin intended to increase water availability to local populations. Between 1961 and 1998, peak discharges were on the order of 3000 $m^3 s^{-1}$, as was the case in 1974. Other significant outflow values are shown in Fig. 2B. After this period, dam construction normalized outflows to average values of approximately 25 $m^3 s^{-1}$, with peak discharges reaching only 255 $m^3 s^{-1}$. As shown in Fig. 2C, the results showed a 10-fold decrease in outflow between the two periods. Dias et al. (2009, 2011) showed, for the Jaguaribe River estuary in June 2006, outflows (Fig. 2C) from the interface between the upper and the middle estuary varying from 5 to 351 $m^3 s^{-1}$ during ebb tide and from 110 to −201 $m^3 s^{-1}$ during flood tide. Measured outflows from the middle to the lower estuary varied from 345 to 1123 $m^3 s^{-1}$ and −771 to −1395 $m^3 s^{-1}$, respectively, during the ebb and flood tides. In years of higher rainfall, those outflows could be an order of magnitude higher (Dias et al., 2009; Marins and Lacerda, 2007; Marins et al., 2003).

In recent decades, few studies have dealt with the basic descriptive oceanography of the continental shelf waters of the Brazilian Northeast. Silva and Alvarenga (1994), in a study conducted over the CSC, observed that salinity shows little seasonal variation, with maximum values (36.2) observed during the spring decreasing from the 100 m isobath toward the surface. They also observed that in the first 70 m, temperature is homogeneous, with minimum values of 25 °C, indicating a barotropic condition over the CSC. Unfortunately, most other studies of the CSC are technical reports of oil and gas exploration companies and are not available for publication.

3. Data sources and methods

3.1. Continental shelf region off the Jaguaribe River

During 2009, two oceanographic cruises (May and November) were conducted over the CSC (Fig. 1A) during the rainy and dry seasons, respectively. Each cruise lasted an average of 10 days and consisted of a total of 16 hydrographic stations distributed in five transects of 3 nautical miles each in the inner shelf region off the mouth of the Jaguaribe River. The middle and external continental shelf regions off the Jaguaribe River were represented by five transects of approximately 25 nautical miles each, totaling 25 hydrographic stations. CTD data (pressure, temperature and salinity) were collected along 10 m isobaths over the inner shelf and along the 10, 20, 30, 50 and 100 m isobaths over the middle and outer shelf. Based on calibration data, the final precisions of the CTD data were ± 0.05 salinity and ± 0.02 °C. The sampling rate of the CTD was 15 Hz. The data for the fluvial contribution were obtained according to Dias et al. (2011), in which synoptic measurements were performed using ADP profiles over the CSC.

To proceed with the analysis of the horizontal and vertical variation fields of the thermohaline structure and the distribution of water masses present in the CSC area, the data were subjected to quality control. To detect and eliminate spurious data, a Gaussian filter based on the gradient of each property was adopted, establishing a maximum range of variation for each property and eliminating any value that exceeded that range. We obtained property profiles in blocks of 1 m from the surface to the bottom and eliminated any values larger or smaller than three times the standard deviation of each block.

Seeking to ensure the same sampling rate at each depth, an average was calculated for each 1 m depth, resulting in vertical profiles with a consistent number of samples. The third and final stage of the basic treatment of the CTD data was a moving-window filtering. These procedures recalculated the values of temperature and salinity for each meter of the water column. The values were replaced by weighted averages between themselves and adjacent values. The number of adjacent values included in this type of average corresponds to the window size used, and the distribution of weighting in relation to the central value is determined by the type of window used. The type of moving window used was the Hanning window, which promotes a weight distribution of Gaussian characters, emphasizing the central average. The elimination of spurious data was realized by removing values greater than three times the standard deviation of each mean (Emery and Thomson, 1998) but should be used cautiously to avoid obscuring significant property gradients. Density was calculated using the conventional associated parameter defined by $\sigma_t = [\rho(S,T) - 1] \times 10^3$, usually expressed in kg m^{-3}.

After the pre-processing of the CTD data, two orthogonal grids were constructed: the first for the inner shelf region, with a resolution of 100×100 m^2 and the second for the middle and outer shelf region, with a resolution of 300×300 m^2 (Fig. 3). The orthogonality of the grids was maintained because the scalar product between two vectors (x, y) was zero. Using these grids, the CTD data were interpolated using a statistical technique called objective analysis (O.A.).

The term O.A. applied to geophysical fluid dynamical data has come to mean an estimation of a scalar or vector field from data by an application of the Gauss–Markotvh theorem (Bretherton et al., 1976; Gandin, 1965). This theorem provides an expression for the minimum quadratic error estimate for a physical variable (salinity or temperature) through which the statistics of a field are estimated in the form of a space-time spectrum. The error maps produced are obtained by the estimation of average quadratic errors of interpolation (Emery and Thomson, 1998).

The O.A. applied in the present study was used as an optimum interpolation in which each estimated average was equal to its real average, and variance was minimized. Carter and Robinson (1987) showed that O.A. corresponds to a linear fit by least squares in which the weight functions depend on the correlations between the data and the grid points. We used a correlation function corresponding to the anisotropic Gaussian correlation function

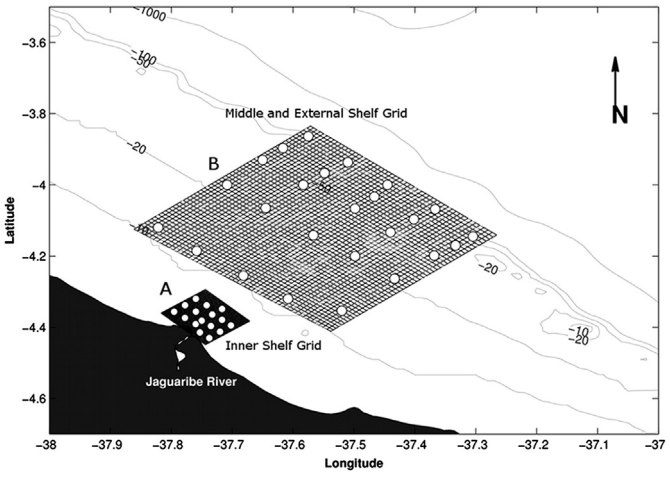

Fig. 3. Sampling grids for the continental shelf area of Ceará State. The white dots represent hydrographic stations.

Table 1
Horizontal areas of the plan of the stations, for the depth of 100 m in each of the cruises.

Cruise	Location	Total area (km^2)	Number of stations	Area by stations (km^2)
Dry seasons	Inner shelf	59.3	16	3.7
	Middle and external shelf	1683.6	25	67.3
Rainy season	Inner shelf	59.3	16	3.7
	Middle and external shelf	1683.6	25	67.3

described by Silveira et al. (2004), according the O.A. requirements described by Carter and Robinson (1987).

During recent decades, the analysis of water masses has taken two main directions. The first is the study of ocean and continental shelf water masses based on the observed correlation of *TS* properties, whereas the second is based on the creation of analytical theories for analysis of *TS* curves. Therefore, we constructed a *TS* spread diagram, in which the plane *T*–*S* represented the observed water distributions using predetermined intervals of salinity and temperature (Miranda, 1982, 1985). Thus, the area of performance for each *TS* pair was set according to its depth and grid point (Fig. 3). To estimate the horizontal area of influence of a given *TS* pair, the area of the grid was divided by the total number of stations in the grid to emphasize the continental shelf (Table 1).

The vertical distance between each *TS* pair was defined according to the following equation:

$$di = \begin{cases} \frac{h_{i+1}-h_i}{2} & \text{se} \quad i=1 \\ \frac{h_{i+1}-h_{i-1}}{2} & \text{se} \quad 1<i<n \\ z-h_i+\frac{h_i-h_{i-1}}{2} & \text{se} \quad i=n \end{cases} \tag{1}$$

where the index i represents the ith observation in the water column, numbered consecutively from the free surface to the bottom ($i=1$ is the observation nearest the surface, and $i=n$ is the observation closest to the bottom), d_i represents the vertical distance of influence of the ith observation in the water column, $h_i \geq 0$ is the depth of the ith observation, n is the number of observations in the vertical dimension for each the oceanographic station, and z is the local station depth (Miranda and Castro, 1979).

After establishing the thermohaline indices for the each water type based on the distribution of *TS* pairs in the *TS* spread diagram, the mixing triangle method initially described by Mamayev (1975) was used. The mixing triangle is utilized to obtain the percentage of each water type present in a representative sample of a mixture in the stationary condition. In the continental shelf waters and particularly in shallow layers, the properties of temperature and salinity are not stationary. Nevertheless, this method was used considering that the time scales involved in the variations of temperature and salinity were larger than the durations of the hydrographic cruises.

The application of this method requires the identification of thermohaline indices (T_1,S_1, T_2,S_2 and T_3,S_3), which is usually performed using the *T*–*S* spread diagram. The percentage quantities of each water type (m_1, m_2, m_3) in a given sample with the temperature T and salinity S are obtained by resolution of the linear system illustrated in the following equation:

$$\begin{aligned} m_1T_1 + m_2T_2 + m_3T_3 &= mT \\ m_1S_1 + m_2S_2 + m_3S_3 &= mS \\ m_1 + m_2 + m_3 &= 1 \end{aligned} \tag{2}$$

The climatology of the percentages of water masses was obtained from *TS* pairs for each grid point using a set of thermohaline indices for coastal and continental waters: River Water (RW), Coastal Water (CW), and for the masses of ocean water, Tropical Water (TW). However, the mixing triangle method becomes invalid for *TS* pairs located outside the triangle (especially those located within the mixed layer); a correction criterion was established for use with percentages that presented negative values. The criterion used was a simple adjustment of the percentages so that they were confined to the range 0–1, thus avoiding loss of information for some of the grid points and possible distortion of the final computed fields.

3.2. Jaguaribe River estuary

For the Jaguaribe river estuary, CTD data were collected during 13 h in two profiles during the dry and rainy seasons (white lines show the locations in Fig. 1B). The locations chosen for the measurements were at the interfaces between the tidal river zone (ZR) and the mixing zone (ZM) (contributing outflow from the upper to the middle estuary) and between the mixing zone (ZM) and the coastal zone (ZC) (contribution outflow from the middle to the lower estuary) (Fig. 1B), according to the criteria adopted by Miranda et al. (2002) and described by Dias et al. (2009) for the Jaguaribe River. The calibration of the CTD was the same as was adopted for the sampling over the continental shelf, the only difference being the sampling rate, for which the CTD was maintained at a fixed position for 1 min at every 25 cm increment of depth in the water column for data acquisition. During the 13 h of sampling, two hydrographic stations were monitored, covering the left and right margins. For each hydrographic profile, a distance of 250 m between stations was observed.

During the preprocessing process, spurious data were detected and eliminated by adopting a filter based on the gradient of each property, as was performed for the continental shelf data. After the CTD data preprocessing stage, we investigated the depth profiles in blocks of 1 m from the surface to the bottom, eliminating values that were larger or smaller than three times the standard deviation of each block (Emery and Thomson, 1998). Seeking to ensure the same sampling rate at each depth, we calculated an average for each 0.25 m of depth, resulting in vertical profiles with a consistent number of samples.

Due to the shallowness of the water column at the hydrographic stations (depths between 3.0 and 8.0 m at slack low and high tides), the sampling depth (z) was normalized according to the method of Kjerfve (1979) using the dimensionless value $Z=z/h(t)$, where $h(t)$ is the water depth at the sampling time. The hydrographic properties (S, T) were interpolated along the water column at intervals of 0.1(Z). The main characteristics of time variations and scalar properties were described at the surface ($Z=0$) and near the bottom ($Z=1.0$) in an ebb and flood tidal regime (Miranda, 1998, 2002).

The numerical integrations for computing the averages in space and time were calculated according to the following equations:

$$\overline{P(t)} = \frac{1}{h}\int_0^h P(z,t)dz = \int_0^1 P(Z,t)dZ \tag{3}$$

$$< P(Z_j) > \; = \frac{1}{T}\int_0^T P(Z_j,t)dt \tag{4}$$

where $P_{(z,\,t)}$ $[P(Z,t)]$ is any scalar property; $P(t)$ denotes its average value in the water column (h) and $< P(Z_j) >$ is the time average of the property at depth Z_j and in the time interval T; as this interval corresponds to one or more tidal cycles, $\langle P(Z_j)\rangle$ simulates the quasi-stationary value of the property. After the CTD data were interpolated according to the dimensionless depth metric, the data were subjected to the O.A., which in the present study, was used as an optimum interpolate second Carter and Robinson (1987).

In estuaries, CW is measurably diluted by RW, and only these two types of water masses are normally observed. Therefore, to calculate the influence of these two water masses, we used a conservative mixing analysis to obtain the percentage of each water type present in a given representative mixture sample in the stationary condition. The application of this method also requires the identification of the thermohaline indices (T_1,S_1 and T_2,S_2), which is usually performed using the T–S spread diagram. The percentage quantities of each water type (m_1 and m_2) in a sample with temperature T and salinity S are obtained by the resolution of the linear system described in the following equation:

$$\begin{aligned} m_1T_1 + m_2T_2 &= mT \\ m_1S_1 + m_2S_2 &= mS \\ m_1 + m_2 &= 1 \end{aligned} \quad (5)$$

Measured outflows of the Jaguaribe River estuary were obtained synoptically using CTD measurements performed over the Continental Shelf to aid in characterizing the continental influences over the CSC. The outflows were obtained by using an acoustic current meter (ADP, 1500 kHz, SONTEK/YSI). Unlike conventional current meters, ADPs measure current profiles by using three sound beams to determine velocity in three dimensions. Thus, ADP measures not only horizontal velocity, as do conventional current meters, but also a vertical component (Gordon, 1989). The size of the vertical cell used was 25 cm. Measurements were performed along a cross section of the Jaguaribe River at the interfaces between the upper and the middle estuary and between the middle and the lower estuary, where the river discharges into the sea. These sections were chosen according to the variation of the estuarine mixing zone, representing the contribution of the drainage basin to the estuary, and the estuary's entry to the adjacent coastal zone (Miranda et al., 2002). Hourly profiles were performed over a period of 12 h during the four transects. Vertical and horizontal velocities were recorded every five seconds within a range of 0.1 to 1.000 cm s^{-1}, with a precision of $\pm 1\%$ for the horizontal velocity and a resolution of 0.1 cm s^{-1} (Cacchione and Drake, 1982; Polonichko et al., 2000; Zedel et al., 1996).

4. Results and discussion

4.1. Thermohaline and mass distributions over the shelf and in the Jaguaribe estuary

During the study period, the largest contributions from the Jaguaribe River to the continental shelf were observed during the rainy season, with values of 1500 m^3 s^{-1} at the interface between the upper and middle estuary regions and 2500 m^3 s^{-1} at interface of the middle and lower estuary regions. However, the outflows observed during the dry period at the interface of the upper and middle estuary regions were 207 m^3 s^{-1} during ebb tide and −360 m^3 s^{-1} during flood tide, whereas at the interface between the middle and lower estuary regions during ebb and flood tides, measured outflows were 403 m^3 s^{-1} and −900 m^3 s^{-1}, respectively. The outflows observed showed the result of the large volume of rainfall in the region during the study period and did not reflect the historical average values shown in Fig. 2.

The variability of the temperature, salinity and density (*TSD*) values observed during the two cruises are presented in Table 2. During the higher fluvial discharge to the inner shelf during the rainy season, temperatures varied from 28.80 to 29.69 °C and were associated with relatively large salinity and conventional density amplitudes that varied from 23.90 to 34.39 and 13.69 to 21.64 kg m^{-3}, respectively. During the dry season, temperatures varied between 27.53 to 27.92 °C and salinity and conventional density variations showed lower amplitudes, from 35.52 to 36.82 and 22.85 to 22.91 kg m^{-3}, respectively. During the rainy season, the *TSD* of the inner shelf showed greater variation compared with the dry period, showing a greater influence of continental waters on the inner shelf during this period that was corroborated by the outflow data simultaneously observed in the estuary.

Table 2
Range, average and standard derivation of salinity, temperature (°C) and conventional density (kg m^{-3}) for the inner, middle and external shelf. STD is the standard deviation. *T* is the temperature, *S* is the salinity and *D* is the conventional density.

		Minimum	Maximum	Mean	STD
Inner shelf					
Rainy season	*T*	28.80	29.69	29.05	0.1
	S	23.90	34.39	32.99	0.9
	D	13.69	21.64	20.54	0.7
Dry season	*T*	27.53	27.97	27.68	0.2
	S	35.52	36.82	36.73	0.2
	D	22.85	22.91	23.80	0.1
Middle and external shelf					
Rainy season	*T*	24.57	28.62	28.04	0.3
	S	35.20	36.50	35.53	0.1
	D	22.37	24.55	22.78	0.1
Dry season	*T*	24.94	27.50	27.00	0.1
	S	35.32	36.46	36.25	0.1
	D	22.95	24.38	23.66	0.1

In the middle and external continental shelf regions, the largest *TSD* amplitudes were observed during the rainy season, with values from 24.57 to 28.62 °C, 35.20 to 36.50 and 22.37 to 24.55 kg m^{-3}, respectively. During the dry season, the *TSD* values varied from 24.94 to 27.50 °C, from 35.32 to 36.46 and from 22.95 to 24.38 kg m^{-3}, respectively. However, the fluvial contribution that was observed in the inner shelf region was not observed in the middle and outer shelf regions.

For the Jaguaribe River estuary sampling performed during the rainy period, there was a large volume of fluvial water that resulted in salinities with values lower than the practical scale (approximately 0.15) and temperatures varying from 29.5 to 30.2 °C and 29.3 to 30.3 °C for the interfaces of the upper and middle estuary and the middle and lower estuary regions, respectively. The larger volume of freshwater found in the estuarine region corroborated the salinity and temperature values observed in the inner shelf region. However, during the dry period at the interface of the upper and middle estuary regions, salinity and temperature varied during the ebb tide from 2.7 to 15.9 and 28.1 to 28.9 °C, whereas during the flood tide they varied from 3.0 to 17.4 and 29.1 to 29.9 °C, respectively. The conventional density varied from 1 to 7 kg m^{-3} during the ebb and flood tides. For the interface of the middle and lower estuary regions, the *TSD* fields varied during the ebb tide from 27.1 to 29.0 °C, 15.2 to 35.6 and 7.3 to 23.1 kg m^{-3}, respectively. During the flood tide, the *TSD* variation was from 27.9 to 29.2 °C, 21.2 to 36.7 and 11.9 to 23.7 kg m^{-3}, respectively. We could observe during the dry season a stronger penetration of the marine waters into the estuarine system resulting from the lower freshwater input from the drainage basin to the estuarine system.

4.2. TS diagram of the continental shelf and Jaguaribe estuary regions

Based on the characteristics observed during the cruises, it was possible to identify three water masses in the study area according to the criteria presented in Table 3. The spatial distributions of the water masses were identified from the three-dimensional locations of their respective limiting isopycnic values (σ_θ). In this case, the isopycnic $\sigma_\theta \leq 21$ delimits the RW influence, and the boundary between CW and TW is marked by the isopycnic $\sigma_\theta = 23.5$. These values were defined based in the classical range defined in

literature (Castro and Miranda, 1998; Da Silva et al., 2005; Miranda, 1982, 1985).

The water masses were defined according to the *TS* diagram that was generated from the correlations between temperature (*T*) and salinity (*S*) data. Fig. 4 shows the *TS* diagram obtained using the water column temperature and salinity data from the hydrographic stations sampled in the inner, middle and outer shelf regions during the rainy (Fig. 4A) and dry (Fig. 4B) seasons. The RW in the study area was identified by temperatures lower than 29 °C and salinity less than 30, characterizing it as typical estuarine water derived from the mixture of sea water with fluvial water, and was located over the inner shelf and in the estuarine channel. The CW was characterized by temperatures ranging between 28 and 29 °C and salinities lower than 36, as a result of the greater influence of marine waters in the study area, and extended from waters over the inner shelf to the break of the outer shelf. In the oceanic area, just below the CW, we could observe the presence of TW, which in this study, was observed near the 100 m isobath and was characterized by the presence of colder waters (25–27 °C) and higher salinities (36).

For the Jaguaribe River during the rainy period (Fig. 4C) we could observe the presence of river water masses (RW) occurring in all samples restricted to isopycnic 5 ($\sigma_\theta \leq 5$) due to the high volume of freshwater mentioned above. However, during the dry period, with water of marine origin being measurably diluted in the estuarine channel, we observed that the fluvial contribution was restricted the isopycnic 5 ($\sigma_\theta \leq 5$), and between isopycnics 5 and 20 ($5 \geq \sigma_\theta \leq 20$) there was a mixture of river water mass (RW) with coastal water mass (CW). Beyond isopycnic 20 ($\sigma_\theta \geq 20$), there was a marked presence of the coastal water masses (CW). This type of distribution was described by Miranda et al. (1998, 2002, 2005) as a classical distribution of water masses in estuarine systems.

Table 3
Values of temperature (°C) and salinity characteristics of the respective water masses observed in the study area.

Water masses	Temperature (°C)	Salinity
River Water (RW)	≤29	≤30
Coastal Water (CW)	28–29	34.5–36
Tropical Water (TW)	25–27	> 36

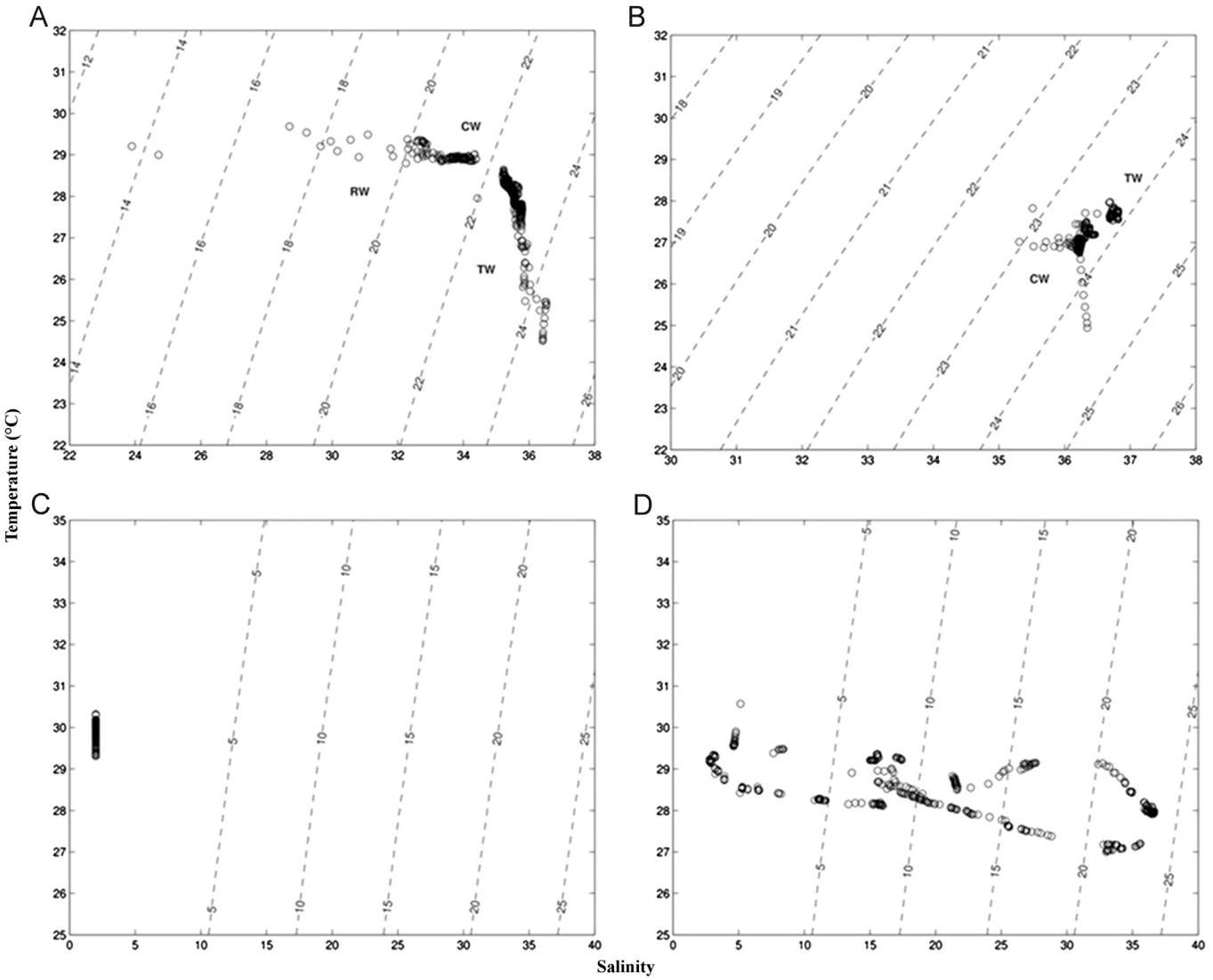

Fig. 4. *TS* diagram from the data collected during two cruises over the CSC and in the Jaguaribe River estuary during the rainy and the dry seasons. (A and B) Continental shelf during rainy and dry periods. (C and D) Jaguaribe River estuary during rainy and dry periods.

4.3. Water masses in the Jaguaribe estuary and continental shelf

Figs. 5 and 6 show the depths and limits of the spatial distributions of the water masses (RW, CW and TW) found over the CSC during the rainy and dry seasons, respectively. During the period of maximum discharge of the Jaguaribe River, one could observe the influence of the river water mass (RW) throughout the superficial part of the dominance (Fig. 5A). Towards the bottom, we observed the presence of the coastal water (CW) that ranged from the subsurface (Fig. 5B) to the bottom (Fig. 5C) but still under the influence of the RW. In the river plume region, the influence of the continental water was observed and a diminution of the CW relative to the RW (Fig. 7A). Miranda et al. (2002) characterized the entry of fluvial water into an adjacent continental shelf region as an estuarine plume. The estuarine plume observed over the inner shelf off the Jaguaribe River penetrated approximately 2 m deep in the water column, but its influence was observed from the surface to the bottom (Fig. 7A).

During the dry season, there was a strong influence of the CW (Fig. 5D–F) with no RW over the inner shelf. This result was corroborated by the vertical distribution of the water masses, shown in Fig. 7B, showing a broad dominance of the CW during this period. This time of the year coincided with the period of reduced river discharges when the trade winds pushed the ITCZ into the northern hemisphere. We could observe that during the period of maximum outflow of the Jaguaribe River, the freshwater discharges were confined to the frontal area of the river mouth, reaching a depth of 2 m, promoting a significant subsidence of the top of the coastal water (CW) over the inner continental shelf reaching to 6 km from the coastline. At this time of the year, the northeast trade winds were almost perpendicular to the isobaths, pressing the plume along the coast, thus reducing its lateral expansion.

The water mass distributions during the rainy season over the middle and outer shelf are shown in Fig. 6A. We could observe a strong presence of the CW in the upper 30 m. The 30–50 m isobath was characterized by the presence of the TW, but its presence was restricted to the region of the continental shelf break (50 and 100 m isobaths). During the dry period (Fig. 6B), there was a well-established presence of the TW in the same region observed during the rainy season. However, there was a major influence of the TW mixed with the coastal water (CW) that could be observed in the upper 30 m. The distributions of the coastal and tropical water masses showed an elevation of the top of the TW on the shelf break that was restricted to the 50–100 m isobath area during the rainy period (Fig. 7C), associated with an increased influence of the TW over the middle continental shelf where the mixture of the CW and TW was observed from a 70 m depth to the surface during the dry period (Fig. 7D).

Fig. 7 shows the vertical distributions of the water masses in two depth profiles performed in the center of each grid for the inner shelf (Fig. 3 profile A), middle and outer shelf (Fig. 3 profile B) regions. The results shown in Fig. 7A corroborated the horizontal distribution showed in Fig. 5, in which the presence of the RW directly influenced the first two meters of the water column, and its mixture with the CW was observed from the subsurface to the bottom during the rainy period. During the dry period, the dominance of the CW throughout the grid was observed (Fig. 7B). This behavior was observed during the rainy period in the middle and outer shelf areas where the TW was restricted to between the 50 m and 100 m isobaths (Fig. 7C) and showed a greater capacity to mix with the CW than during the dry season (Fig. 7D).

The results of this study showed the presence of a water mass of continental origin (RW) over the inner shelf that entered the continental shelf at a distance of 6 km from the coastline and had lower salinity (≤30) and temperature 29 °C. The RW was associated with a coastal water mass (CW) that had salinity varying between 34.5 and 36 and temperature between 28 and 29 °C, resulting in the formation during the rainy season of a halocline

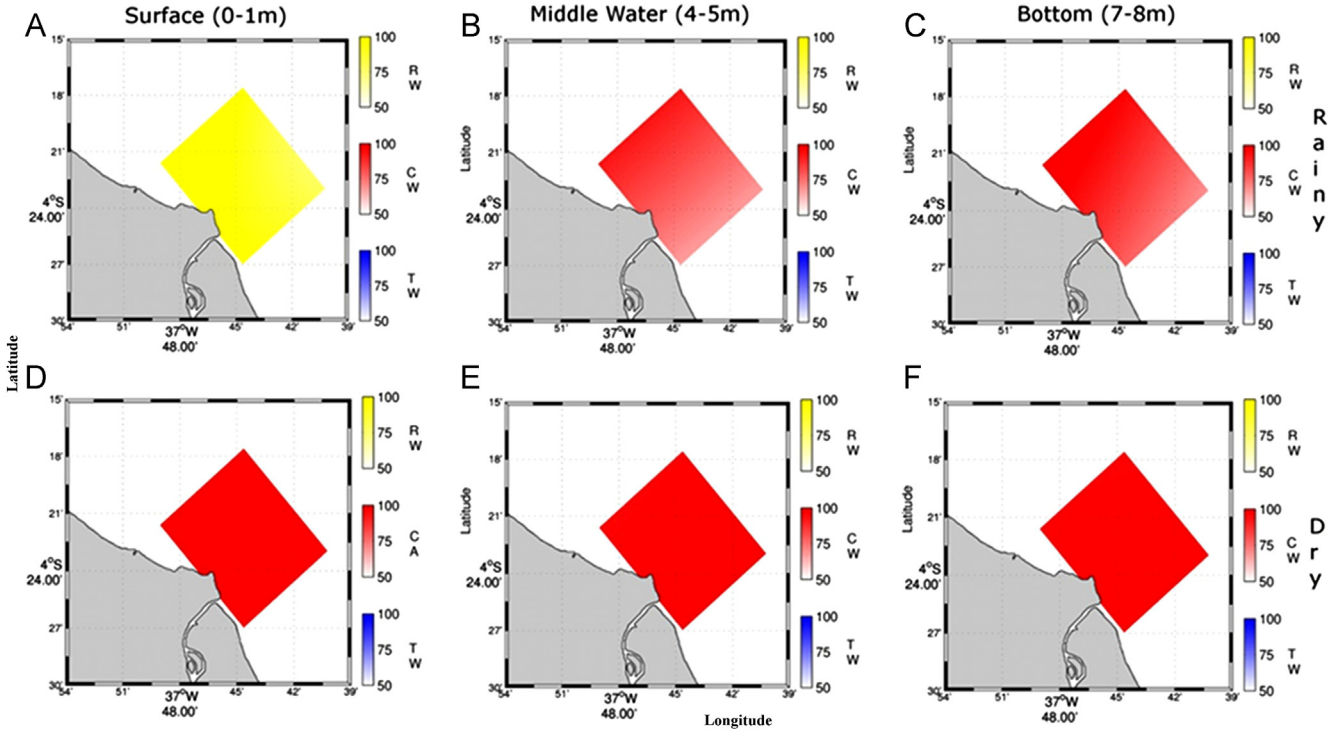

Fig. 5. Distribution of water masses over the inner shelf during the rainy and dry seasons. (A) Water masses at the surface during the rainy season. (B) Water masses in the middle water during the rainy season. (C) Water masses at the bottom during the rainy season. (D) Water masses at the surface during the dry season. (E) Water masses in the middle water during the dry season. (F) Water masses at the bottom during the dry season.

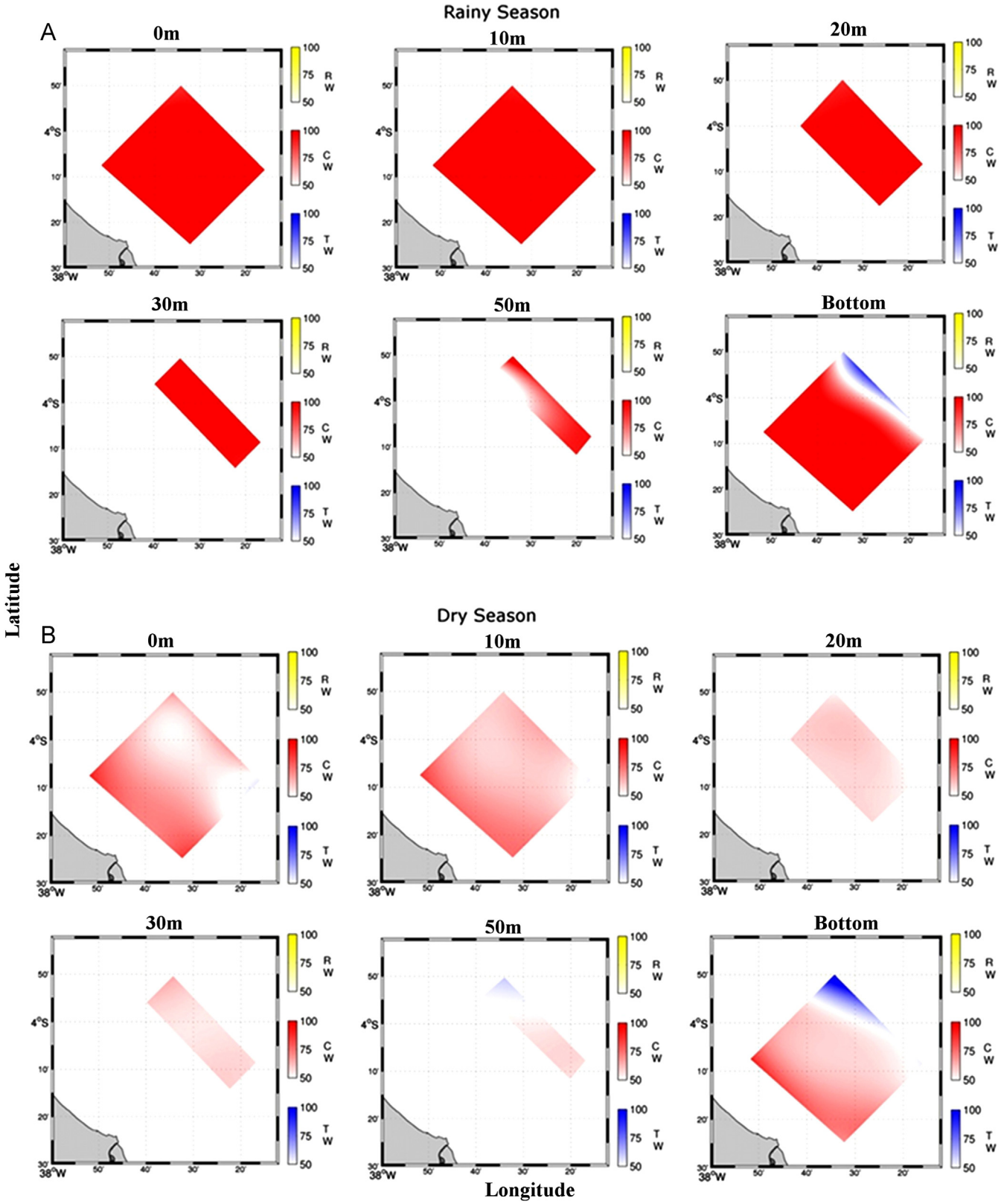

Fig. 6. Horizontal distributions of water masses in the middle and outer shelf areas during the rainy (A) and dry (B) seasons. RW – River Water (yellow bar); CW – Coastal Water (red bar); TW – Tropical Water (blue bar). (For interpretation of the references to color in this figure legend, the reader is referred to the web version of this article.)

observed between the surface and 2 m depth, characterizing the estuarine plume of the Jaguaribe River and a direct reflection of the large continental outflow observed during the period. In the middle and outer shelf regions, the presence of the RW was not observed due to the low river discharge and the action of the northeast trade winds, which tended to imprison this water mass close to the coastline. Over the shelf break, the presence of an oceanic water mass (TW) was observed with high salinity (>36)

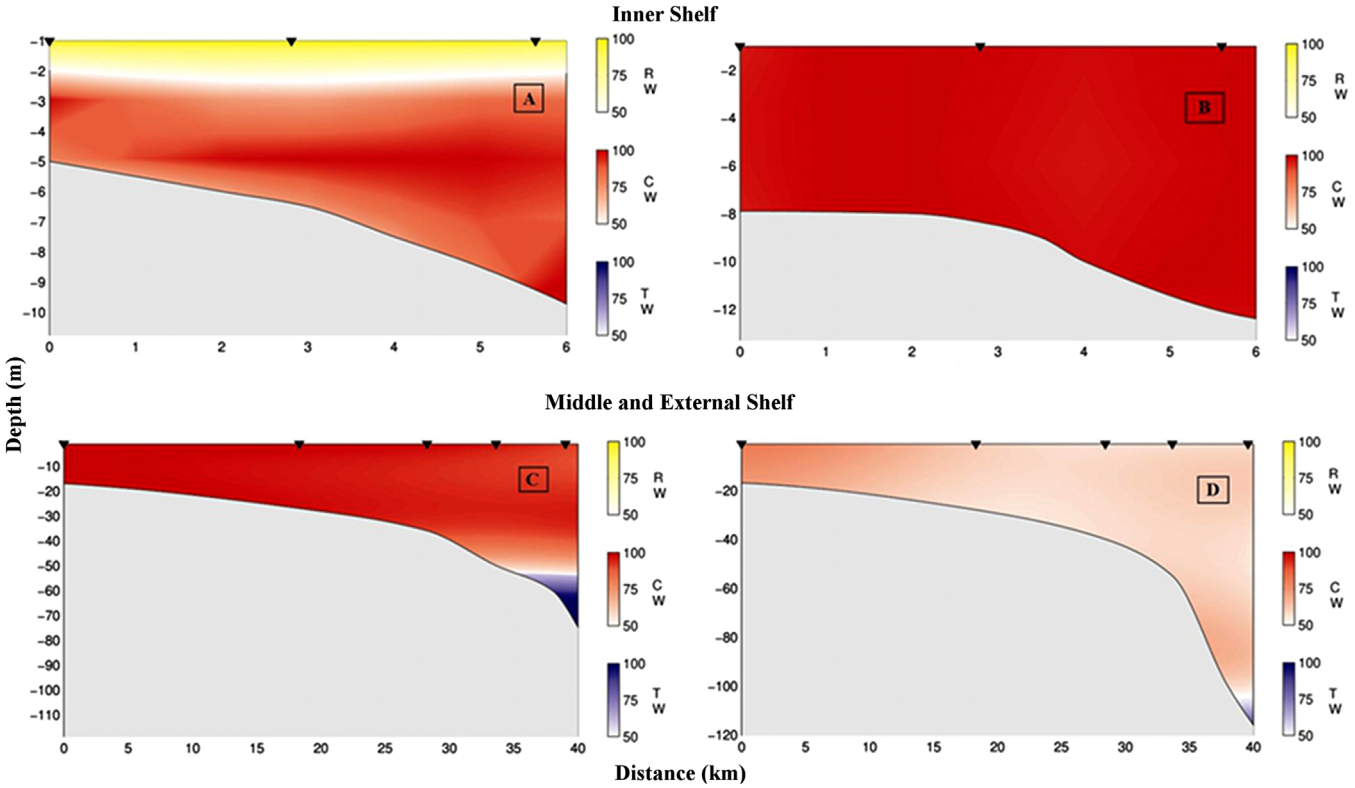

Fig. 7. Vertical distributions of water masses over the inner shelf (profile A) during the rainy (A) and dry (B) seasons and in the middle and outer shelf regions (profile B) during the rainy (C) and dry (D) seasons.

and relatively low temperature (from 25 to 27 °C), but it was restricted to 50 m isobath during the rainy season. During the dry season, the TW showed more intense mixing with the CW.

Studies conducted over the northern and northeastern Brazilian continental shelf have shown the existence of space-time variability in the North Brazil Current (NBC) and the role of the anticyclonic vortex that meanders along the adjacent ocean towards the continental shelf (Schott et al., 1998; Silveira et al., 1994; Stramma and Schott, 1999). The results of these studies showed that the NBC has a large seasonal variability in which, during the rainy season, the NBC remains narrow and confined to the continental slope region of the CSC, carrying approximately 13 Sv (low annual transport). During the dry season, the NBC turns into a boundary current that is larger and deeper, reaching values of transport of approximately 36 Sv (maximum annual transport). The expansion of the TW (elevation of its top and subsidence from its base) observed during the dry season in the middle and external continental shelf areas coincided with the period of maximum transport for the NBC and intense activity of subsurface anticyclonic eddies described in these studies. Marin (2009) observed the presence of mesoscale frontal features with vertical extensions coincident with the extension of the North Brazil Undercurrent (NBUC) that were named Macau eddies by the author. This pattern was easily observed when we compared the depth limits of the CW and TW during the periods of drought and rain. During the rainy season, the TW was restricted to depths greater than 50 m (Fig. 7C), whereas during the dry season, its expansion had a greater influence on the shelf (Fig. 7D).

In the Jaguaribe River estuary, the distributions of the water masses during the rainy and dry seasons are shown in Fig. 8. The information in Fig. 8A and B corroborated the results for the inner shelf during the rainy period in which we could observe the dominance of the RW (higher than 95%) at the interface of the upper and middle estuaries and the interface of the middle and lower estuaries. During this period of the year, the estuarine channel behaved with a unidirectional flow and the estuary was transported out from the coastline, as seen in Fig. 7A. As shown in the *TS* diagram (Fig. 4C and D), during the dry season, there was a relatively great influence of the oceanic water mass in the Jaguaribe river estuary. In the region that receives the direct contribution of the drainage basin (upper and middle estuary interface), one could observe in the event of ebb tide (Fig. 8C) a RW dominance (above 90%), while early in the flood tide we observed a greater mixture of the RW with CW (with percentages higher than 80% and 70%) (Fig. 8D and E). However, in the region that marks the contribution from the estuary to the adjacent ocean (middle and lower estuary interface) it was observed that even in the event of the ebb tide there was no RW dominance, but a mixture between the RW and CW (Fig. 8F). In the event of the flood tide, the region begins to be dominated entirely by the CW, with percentages of 65% (Fig. 8G) and greater than 80% (Fig. 8H).

Fig. 8 shows the behavior of the Jaguaribe estuary during a year of rainfall above the historical average when the dams constructed along its course did not influence either the freshwater input of the drainage basin to the estuary or the input from the estuary to the adjacent ocean during the rainy season (Fig. 8A and B), a behavior previously observed by Dias et al. (2009). However, during the dry period, it was observed that at the interface that receives the direct fluvial contribution (upper and middle estuary interface) there was a dominance of the RW, but during the flood tide, it was observed that an increased influence of the CW generated a mixture between the RW and CW. For the interface that received the contribution from the estuary (middle and lower estuary interface) we could see that the dominance or the mixture of the water masses varied with the fluctuation of the tide during the period, due to a lower influence of river water in the region

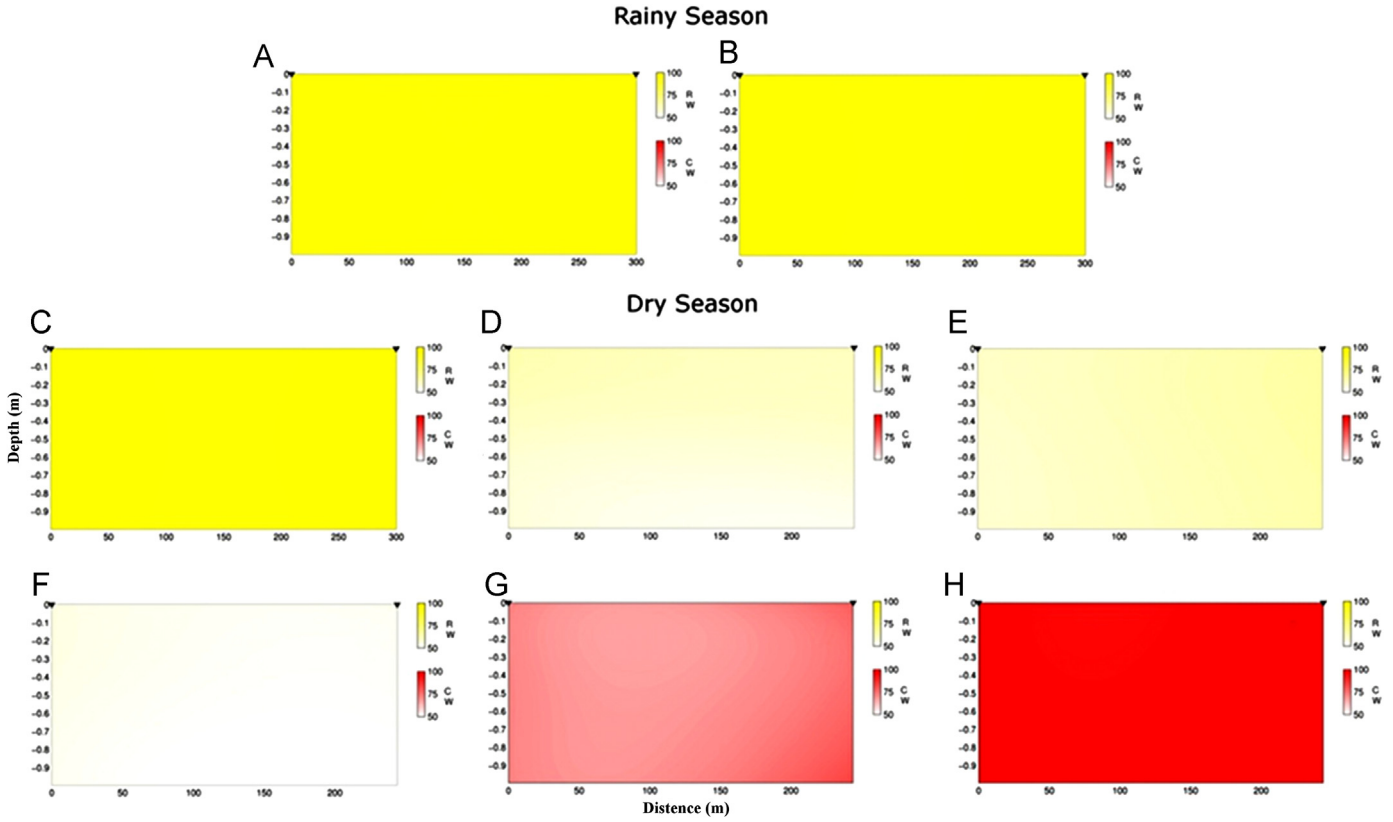

Fig. 8. Distributions of water masses in the Jaguaribe River estuary during the rainy and dry seasons, at the upper and middle estuary and middle and lower estuary interfaces. (A and B) refer to the interfaces of the upper and middle estuary and the middle and lower estuary during the rainy season, respectively. (C–E) refer to the interface of the upper and middle estuary during the dry season over a tidal cycle, and (F–H) refer to the middle and lower estuary interface again during the dry season and over a tidal cycle.

when compared with the distribution observed during the rainy season.

The fronts were characterized as zones in which the intensification of the near-horizontal gradient of one or more physical properties occurred, although often separating water masses of different origins and physicochemical properties. The results presented in this work showed the presence of three fronts in the continental shelf region, as outlined in Fig. 9.

The bottom thermal front (BTF) had been associated with more and less intense intrusions of the water masses transported by the North Brazil Current (NBC) along the continental shelf break in the coastal direction. Silveira et al. (1994) showed that the NBC in its natural drainage on the continental slope transported TW on the surface and SACW in the subsurface of a water column of 600 m. The BTF is formed in the region that separates the relatively cold water, identified as TW, from warmer water characteristic of the inner shelf region, which we call the CW. As a result, the BTF separates, in the deep layer, water of oceanic origin (TW) from water of coastal origin (CW), characterizing the intersection as the bottom of the thermocline.

The spatial and temporal variation of the BTF in the inner limit of PCE suggests that the scale of the intrusion on the TW platform is greater during the dry season. As there are no studies in the CSC literature to explain the seasonal variation of the buoyancy flux due to heat exchange and mass in the atmosphere–ocean interface, we suggest that the location of the BTF is associated with the penetration of colder water coming from the NBC towards the coast.

The surface haline front (SHF), especially during the rainy season, showed the characteristics of the shelf break front, located, for this season, on the Continental Shelf Break (CSB). In the region of the CSB, the SHF delimits the catchment area of two water masses of different origins. The CW is located in the outside region of the front as a result of mixing between CW and TW, whereas the predominance of the continental water mass (RW) is observed on the inside front. Thus, we suggest that the SHF separates ocean waters (TW) from coastal waters (CW) on its outside, and bounds the influence area of the continental water mass (RW) in the IS region on the inside. The variation of the SHF in the region of the CSB depends on the water volume carried by the NBC in the coastal direction or the presence of mesoscale frontal structures in the region. In the IS region, this variation depends on the intensification or minimization of the contribution from the continental drainage.

5. Conclusions

This study examined a number of hydrographic data obtained in the Exclusive Economic Zone of Brazil comprising the eastern portion of the continental shelf of Ceará State and data obtained in the Jaguaribe River estuary, strengthening knowledge about the locations' seasonal variation of the thermohaline structure and the distribution of water masses in that location and characterizing the actual contribution of the freshwater discharge to the continental shelf waters in a poorly researched portion of the Atlantic Ocean.

Analyses of synoptic observations showed that during the period of maximum river discharges, the presence of the RW was dominant, with its influence felt over the inner shelf in the

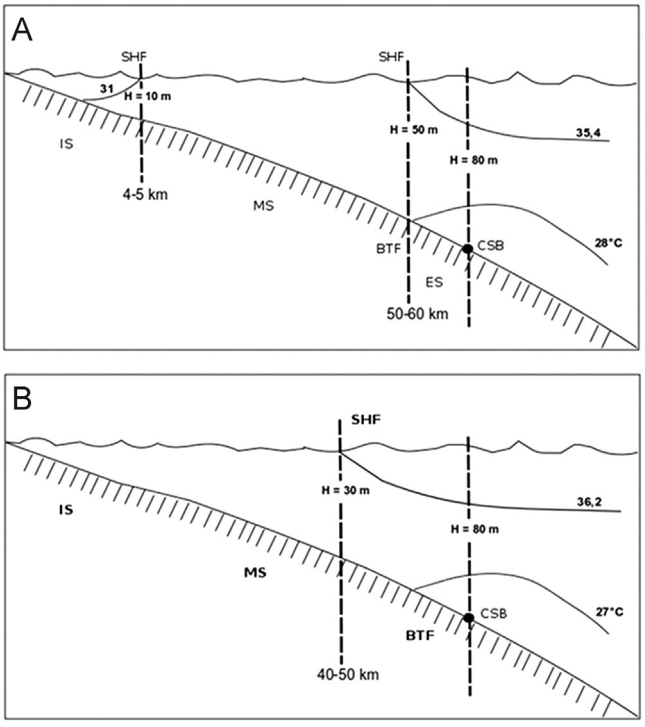

Fig. 9. Schematic representation of the regions of the continental shelf of Ceará during the rainy (top) and dry (bottom) seasons. SHF is the surface haline front, BTF is the bottom thermal front, CSB is the continental shelf break; IS, MS and ES are the inner, middle and external continental shelf regions, respectively. The depths (*H*) are expressed in meters (m) and horizontal distances in kilometers (km).

form of a water plume of low salinity that extended to 6 km off the coastline. The presence of this plume lowered the top of the CW and influenced the mixing of the RW and CW throughout the water column. However, in the middle and external continental shelf regions, the presence of the RW was not observed, most likely due to the increased activity of the northeastern trade winds pressing the plume along the coast, thus reducing its seaward expansion. During this period of maximum continental discharge, the middle and external continental shelf areas showed the presence of the CW and the occurrence of the TW below the 50 m isobath.

During the dry season, the variation of the semidiurnal tide observed in the study region showed a strong influence on the mixing of the water masses (RW/CW) in the estuarine channel of the Jaguaribe River, and these variations were linked to the ebb and flood tide events. In the inner shelf region, a marked presence of the CW was observed, whereas the RW was restricted to the estuarine channel, most likely due to the limited competence of the RW to reach the continental shelf. In the middle and outer shelf regions, a higher influence of the TW was observed, most likely influenced by the existence of space-time variability in the behavior of the NBC and the role of anticyclonic eddies that meander along the adjacent ocean towards the continental shelf. Even in low latitudes, the baroclinic adjustment of the NBC may contribute to TW intrusion on the northeastern continental shelf.

Finally, the results point to the necessity of detailed investigation of the relative importance of river discharge and the intensification of the baroclinic adjustment of the NBC on the variability of the structure of water masses observed over the CSC. In this sense, the mathematical modeling of ocean circulation in the study area appears to be a powerful tool for quantifying the phenomena involved.

Acknowledgments

This study is part of the INCT-TMCOcean (www.inct-tmcocean.com.br): "Continent-Ocean Materials Transfer" project supported by CNPq, Brazil, Process no. 573.601/2008-9 and the ITHATROPICAL (France/CNPq/IRD) project supported by CNPq. The authors also thank the Blue Amazon Program from CAPES for providing grants to FJSD. We extend our deep thanks to the crew of the N.Oc Prof. Martins Filho, who made this work possible and to the Oceanographic Instrumentation laboratory at the University of São Paulo (LIO/IO/USP), especially to engineers Francisco Vicentini and Luiz V. Nonato and to technician Wilson Natal. The authors also thank Dr. Luiz Bruner de Miranda for valuable discussions on the topic under study.

References

ANA, 2008. National Water Agency. Historic Outflows From Jaguaribe River. ⟨www.hidroweb.ana.gov.br⟩ (retrieved 20.10.2008).
Arz, H.W., Patzold, G., Wefer, G., 1999. Climatic changes during the last glaciations recorded in sediment cores from the northeastern Brazilian Continental Margin. Geo-Marine Letters 19, 209–218.
Bindoff, N.L., Rosenberg, M.A., Warner, M.J., 2000. On the circulation and water masses over the Antarctic continental slope and rise between 80 and 150°E. Deep-Sea Research Part II: Topical Studies in Oceanography 47 (12–13), 2299–2326.
Bretherton, F.P., Davis, R.E., Fandry, C.B., 1976. A technique for objective analysis and design of oceanographic experiments applied to MODE-73. Deep Sea Research and Oceanographic Abstracts 23, 559–582.
Cacchione, D.A., Drake, D.E., 1982. Measurements of storm generated bottom stress on the continental shelf. Journal of Geophysical Research 87, 1952–1960.
Carter, E.F., Robinson, A.R., 1987. Analysis models for the estimation of oceanic fields. Journal of Atmospheric and Oceanic Technology 4, 49–74.
Castro, B.M., Miranda, L.B., 1998. Physical oceanography of the western Atlantic continental shelf located between 4°N and 34°S. Sea 11, 209–251.
Cochrane, J.D., Kelly, F.J., Oiling, C.R., 1979. Subthermocline countercurrents in the western Atlantic Ocean. Journal of Physical Oceanography 9 (4), 724–738.
Curtin, T.B., 1986. Physical observations in the plume region of the Amazon river during peak discharge-II. Water masses. Continental Shelf Research 6 (1–2), 53–71.
Curtin, T.B., Legeckis, R.V., 1986. Physical observations in the plume region of the Amazon river during peak discharge-I. Surface variability. Continental Shelf Research 6 (1–2), 31–51.
Da Silva, A.C., Araujo, M., Bourles, B., 2005. Variação sazonal da estrutura de massas de água na Plataforma Continental do Amazonas e área oceânica adjacente. Revista Brasileira de Geofísica 23 (2), 145–157.
Dias, F.J.S., Marins, R.V., Maia, L.P., 2009. Hydrology of a well-mixed estuary at the semi-arid Northeastern Brazilian coast. Acta Limnologica Brasiliensia 21 (4), 377–385.
Dias, F.J.S., Lacerda, L.D., Marins, R.V., Paula Filho, F.C.F., 2011. Comparative analysis of rating curve and ADP estimates of instantaneous water discharge through estuaries in two contrasting Brazilian rivers. Hydrological Processes 25, 2188–2201.
Dominguez, J.M.L., 2004. The coastal zone of Brazil—an overview. Journal of Coastal Research 39, 16–20.
Emery, W.J., Thomson, R.E., 1998. Data Analysis Methods in Physical Oceanography. Pergamon, Oxford.
Emilson, I., 1961. The shelf and coastal waters off southern Brazil. Bulletin of Oceanography, Institute of Sao Paulo University 11 (2), 44–54.
Gandin, L.S., 1965. Objective analysis of meteorological fields. Israel Program for Scientific Translations Jerusalem 92 (393), http://dx.doi.org/10.1002/qj.49709239320.
Garvine, R.W., 1977. River plumes and estuary fronts, Estuaries, Geophysics and the Environment. National Academy of Science, Washington, D.C., pp. 30–35.
Garvine, R.W., Monk, J.D., 1974. Frontal structure of a river plume. Journal of Geophysical Research 79 (15), 2251–2259.
Geyer, W.R., Beardsley, R.C., Candela, J., Castro, B.M., Legeckis, R.V., Lentz, S.J., Limebuerner, L., Miranda, L.B., Trowbridge, J.H., 1991. The physical oceanography of the Amazon outflow. Oceanography 4, 8–14.
Gordon, R.L., 1989. Acoustic measurement of river discharge. Journal of Hydraulic Engineering 115 (7), 925–936.
Kjerfve, B., 1979. Measurement and analysis of water current, temperature, salinity and density. In: Dyer, K.R. (Ed.), Estuarine Hydrography and Sedimentation. Cambridge University Press, Cambridge, pp. 186–226.
Knoppers, B., Ekau, W., Figueiredo, A.G., 1999. The coast and shelf of east and northeast Brazil and material transport. Geo-Marine Letters 19, 171–178.
Kousky, V.E., 1980. Diurnal rainfall variation in northeast Brazil. Monthly Weather Review 108, 488–498.
Mamayev, O.I., 1975. Temperature–Salinity Analysis of World Ocean Waters. Elsevier Scientific, Amsterdam.

Marin, F.O., 2009. The Undercurrent North of Brazil off the Northeastern Coast. Universidade de Sao Paulo, Oceanographic Institute. (Master's thesis), São Paulo, SP.
Marins, R.V., Lacerda, L.D., 2007. Summary of drivers, pressures and environmental impacts in the Jaguaribe River Estuary, NE Brazil. Electronic Journal ⟨www.institutomilenioestuarios.com.br⟩ volume is V1, (accessed 02/07/11).
Marins, R.V., Lacerda, L.D., Abreu, I.M., Dias, F.J.S., 2003. Efeitos da açudagem no rio Jaguaribe. Revista Ciência Hoje 33 (197), 66–70.
Martins, L.R., Coutinho, P.N., 1981. The Brazilian continental margin. Earth-Science Reviews 17, 87–107.
Mascarenhas, J.A.S., Miranda, L.B., Rock, N.J., 1971. A study of the oceanographic conditions in the region of Cabo Frio. In: Costlow Jr., J.D. (Ed.), Fertility of the Sea, vol. 1. Gordon and Breach, New York, pp. 285–308.
Metcalf, W.G., Stalcup, M.C., 1967. Origin of the Atlantic undercurrent. Journal of Geophysical Research 72, 4959–4975.
Miranda, L.B., 1982. Analise de massas de água da plataforma continental e da região oceânica adjacente: Cabo de São Tome (RJ) a Ilha de São Sebastião (SP). Tese de Livre-Docência. Instituto Oceanográfico, São Paulo.
Miranda, L.B., 1985. Forma da correlação T–S de massas de água das regiões costeira e oceânica entre cabo de São Tome (RJ) e a Ilha de São Sebastião (SP). Boletim do Instituto Oceanografico 33 (2), 105–119.
Miranda, L.B., Castro, B.M., 1979. Aplicação do diagrama T–S estatístico volumétrico a analise das massas de água da plataforma continental do Rio Grande do Sul. Boletim do Instituto Oceanografico 28 (1), 185–200.
Miranda, L.B., Bergamo, A.L., Castro, B.M., 2005. Interactions of river discharge and tidal modulation in a tropical estuary, NE Brazil. Ocean Dynamics 55 (5–6), 430–440, http://dx.doi.org/10.1007/s10236-005-0028-z.
Miranda, L.B., Castro, B.M., Kjerfve, B., 1998. Circulation and mixing in the Bertioga Channel (SP, Brazil) due to tidal forcing. Estuaries 21 (2), 204–214.
Miranda, L.B., Castro, B.M., Kjerfve, B., 2002. Princípios de Oceanografia Física de Estuários. Edusp, São Paulo.
Molinari, R.L., 1982. Observations of eastward currents in tropical South Atlantic Ocean: 1978–1980. Journal of Geophysical Research 87, 9707–9714.
Molinari, R.L., 1983. Observations of near-surface currents and temperature in the central and western tropical Atlantic. Journal of Geophysical Research 88, 4433–4438.
Okunda, T., 1962. Physical and chemical oceanography over continental shelf between Cabo Frio and Vitoria (central Brazil). Journal of the Oceanographical Society of Japan 1, 514–540.
Peterson, R.G., Stramma, L., 1990. Upper level circulation in the South Atlantic Ocean. Progress in Oceanography 26 (1), 1–73.
Polonichko, V., Mullison, J., Cabrera, R., 2000. Pulse-coherent acoustic Doppler profiler. Sea Technology 1 (2), 76–78.
Riehl, H., 1965. Meteorologia Tropical. Tradução Aurélio Augusto da Rocha. Missão Norte-Americana de Cooperação Econômica e Técnica no Brasil, Rio de Janeiro.
Schott, F.A., Fischer, J., Stramma, L., 1998. Transports and pathways of the upper-layer circulation in the western tropical Atlantic. Journal of Physical Oceanography 28, 1904–1928.
Silva, L.C.F., Alvarenga, J.B.R., 1994. Levantamento do estado da arte dos recursos vivos marinhos do Brasil—Oceanografia Física da Região Nordeste. Ministério do Meio Ambiente, Brasilia – DF.
Silveira, I.C.A., Miranda, L.B., Brown, W.S., 1994. On the origins of the north Brazil current. Journal of Geophysical Research 99 (c11), 22501–22512.
Silveira, I.C.A., Calado, L., Castro, B.M., Cirano, M., Lima, J.A.M., Mascarenhas, A.S., 2004. On the baroclinic structure of the Brazil current-intermediate western boundary current system. Geophysical Research Letters 31 (14), L14.308.
Soares, J.R., Castro Filho, B.M., 1996. Numerical modeling of the response of Ceará Continental shelf waters to wind stress forcing. Revista Brasileira de Oceanografia 44 (2), 135–153.
Stramma, L., Schott, F., 1999. The mean flow field of the tropical Atlantic Ocean. Deep-Sea Research Part II: Topical Studies in Oceanography 46, 279–303.
Summerhayes, C.P., Coutinho, P.N., França, A.M.C., Ellis, J.P., 1975. Upper continental margin sedimentation of Brazil: Salvador to Fortaleza, Northeastern Brazil. Contributions to Sedimentary Geology 4, 44–77.
Zedel, L., Hay, A.E., Cabrera, R., Lohrmann, A., 1996. Performance of a single-beam pulse-to-pulse coherent Doppler profiler. Journal of Oceanic Engineering 20, 290–297.